Passive ultrasonics using sub-Nyquist sampling of high-frequency thermal-mechanical noise

Karim G. Sabra, Justin Romberg, Shane Lani, et al.

Citation: The Journal of the Acoustical Society of America **135**, EL364 (2014); doi: 10.1121/1.4879666
View online: https://doi.org/10.1121/1.4879666
View Table of Contents: https://asa.scitation.org/toc/jas/135/6
Published by the Acoustical Society of America

Passive ultrasonics using sub-Nyquist sampling of high-frequency thermal-mechanical noise

Karim G. Sabra[a)]
School of Mechanical Engineering, Georgia Institute of Technology, 771 Ferst Drive, Atlanta, Georgia 30332-0405
karim.sabra@me.gatech.edu

Justin Romberg
School of Electrical and Computer Engineering, Georgia Institute of Technology, 777 Atlantic Drive NW, Atlanta, Georgia 30332-0250
jrom@ece.gatech.edu

Shane Lani and F. Levent Degertekin
School of Mechanical Engineering, Georgia Institute of Technology, 771 Ferst Drive, Atlanta, Georgia 30332-0405
lani.shane@gatech.edu, levent.degerteking@me.gatech.edu

Abstract: Monolithic integration of capacitive micromachined ultrasonic transducer arrays with low noise complementary metal oxide semiconductor electronics minimizes interconnect parasitics thus allowing the measurement of thermal-mechanical (TM) noise. This enables passive ultrasonics based on cross-correlations of diffuse TM noise to extract coherent ultrasonic waves propagating between receivers. However, synchronous recording of high-frequency TM noise puts stringent requirements on the analog to digital converter's sampling rate. To alleviate this restriction, high-frequency TM noise cross-correlations (12–25 MHz) were estimated instead using compressed measurements of TM noise which could be digitized at a sampling frequency lower than the Nyquist frequency.

PACS numbers: 43.35.Yb, 43.60.Qv, 43.60.Ek [DC]
Date Received: January 18, 2014 **Date Accepted:** April 25, 2014

1. Introduction

Broadband thermal-mechanical (TM) noise in electromechanical systems is ubiquitous but rarely exploited. However, TM noise can be considered as a fully diffuse noise field, especially for very high-frequency ultrasonics ($f > 10$ MHz). Consequently, the cross-correlation of TM noise recorded by two ultrasonic sensors can be used to passively estimate the ultrasonic waves propagating between them (i.e., Green's function).[1–4] This provides a foundation for high-frequency passive ultrasonics without active transmitter elements. Furthermore, since the TM noise has low amplitude and there is no active transmitter to create a dead zone in the images (caused by amplifier saturation and nonlinear effects), high-frequency passive ultrasonic imaging can potentially enable very high resolution (i.e., low *F*-number) images at distances limited only by the near field of the ultrasonic array elements.[4]

Implementing this high-frequency passive ultrasonics approach is contingent upon two main constraints. First, the array elements need to have a very low self-noise to record the weak TM noise field while having a sufficiently small size to ensure high-resolution at high frequencies. Preliminary results indicate that capacitive

[a)]Author to whom correspondence should be addressed.

micromachined ultrasonic transducers (CMUTs) with low noise electronics can fulfill these sensor requirements.[4,5] Second, getting accurate and synchronous recordings of very high-frequency TM noise (e.g., up to 100 MHz) on multiple sensors put stringent requirements on the analog to digital converters (ADCs). But, such requirements may be beyond the sampling rate limitations of most commercially available and affordable ADCs. However, recent studies from the field of compressive sampling have shown that signal reconstruction and parameter estimation (e.g., via matched-filtering) are possible by processing compressed (or encoded) versions of the sensor's analog output, which can then be digitized at a much lower sampling frequency than the conventional Nyquist sampling frequency.[6,7] This type of encoding hardware has been implemented for signal bandwidths in the GHz range.[8,9] Based on this approach, this article demonstrates the feasibility of high-frequency—and thus high-resolution—passive ultrasonics by estimating TM noise cross-correlations directly from compressed versions of CMUT measurements of TM noise. This approach could facilitate the practical development (e.g., sensor integration or electronic packaging) of passive ultrasonics by using readily available low sampling rate ADCs, which are usually robust and low-power.

2. Theory

Passive ultrasonics relies on computing the cross-correlation of TM noise recordings $x_1(t)$ and $x_2(t)$ obtained by a pair of sensors 1 and 2 (Refs. 4 and 10),

$$\bar{R}_{12}(t) = \frac{1}{T}\int_0^T x_1(\tau)x_2(\tau+t)d\tau, \tag{1}$$

where T is the recording duration. For sufficiently long recording duration T, the conventional estimator $\bar{R}_{12}(t)$ converges towards its expected value, denoted $R_{12}(t)$ hereafter,

$$R_{12}(t) = E_\tau[x_1(\tau)x_2(\tau+t)] = \lim_{T\to\infty}\bar{R}_{12}(t). \tag{2}$$

If the recorded TM noise approximates a fully diffuse noise field, the expected value $R_{12}(t)$ is a good proxy for the pulse-echo (or pitch-catch) waveform obtained when sensor #1 acts as a source and sensor #2 as a receiver; and thus includes all direct and scattered arrivals due to target echoes between sensors 1 and 2.[1–4] Note that in practice the raw analog noise data coming from the sensor pairs are first run through an anti-aliasing filter and digitized at twice the Nyquist frequency f_{Nyq} (e.g., as determined by the effective frequency bandwidth B of sensors 1 and 2) prior to computing Eq. (1). For finite recording duration T, a coherent arrival is only clearly visible from the cross-correlation waveform $\bar{R}_{12}(t)$ when this arrival's amplitude [e.g., see Fig. 1(b)] becomes larger than the peak amplitude of the residual temporal fluctuations which sets the background "noise" level of the waveform $\bar{R}_{12}(t)$. Assuming that these residual temporal fluctuations behave as Gaussian random signals, the variance of the conventional estimator $\bar{R}_{12}(t)$ can be approximated by[10,11]

$$\mathrm{Var}\left(\bar{R}_{12}(t)\right) \approx \frac{\sigma_{x_1}^2\sigma_{x_2}^2}{2TB}, \tag{3}$$

where $\sigma_{x_i}^2$ $(i=1,2)$ represent the variance of the stationary process $x_i(t)$ over the duration T.

We propose here to estimate the expected value of the TM noise cross-correlation between sensors 1 and 2 directly from compressed TM noise measurements acquired at a sampling frequency $f_s < 2f_{\mathrm{Nyq}}$ using a four step procedure outlined hereafter. To do so the analog sensor outputs from both sensors $x_i(t)$ $(i=1,2)$ of duration T, are first run through the same anti-aliasing filter to be lowpass filtered below f_{Nyq}.

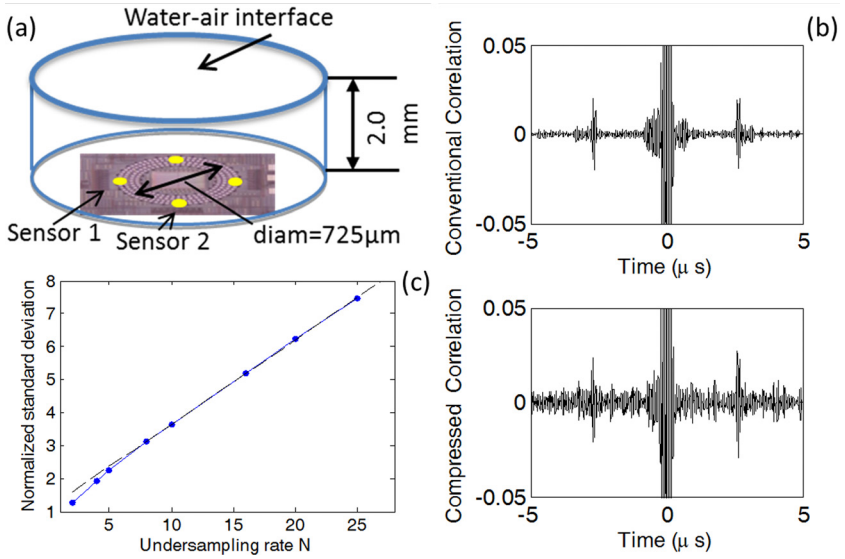

Fig. 1. (Color online) (a) Experimental setup for passive sensing of the water interface with CMUT ring array. (b) Thermal-mechanical noise cross-correlation between sensors 1 and 2 obtained from (upper plot) the conventional estimator $\bar{R}_{12}(t)$ [Eq. (1)] computed from 1 s long noise recordings sampled at $f_{\mathrm{Nyq}} = 100$ MHz or (lower plot) the compressed estimator $\tilde{R}_{12}(t)$ [Eq. (7), with M = 1] using compressed versions of the 1 s long noise recordings sampled at a frequency $f_s = 10$ MHz, i.e., an undersampling rate of $N = 10$. (c) Evolution of the values of the standard deviation (i.e., square root of the variance) of the compressed estimator $\tilde{R}_{12}(t)$, normalized by the value of the standard deviation of the conventional estimator $\bar{R}_{12}(t)$, for increasing values of the undersampling rate N. The number of compressed measurements M is set to 1. The theoretical linear fit predicted by Eq. (17) is indicated as a dashed line.

Second, each analog output $x_i(t)$ is continuously mixed (i.e., multiplied) against a pseudo-random binary function $\mathbf{\Phi}_i(t)$ $(i = 1,2)$ defined by

$$\mathbf{\Phi}_i(t) = \varepsilon_i[q] \text{ for } \frac{(q-1)}{2f_{\mathrm{Nyq}}} \leq t \leq \frac{q}{2f_{\mathrm{Nyq}}} (q = 1 \cdots 2f_{\mathrm{Nyq}} T), \tag{4}$$

where $\varepsilon_i[q]$ is a known sequence of an independent and identically distributed random binary variable that takes values ± 1 with equal probability. Third, the results of these randomized mixings get integrated over a sample period $1/f_s$, which effectively yields a compressed version of the analog noise measurements, denoted y_i $(i = 1,2)$. For instance the kth compressed sample, $y_i[k]$, is given by the inner product between the analog waveform $x_i(t)$ and the known random function $\Phi_i(t)$ over the time period $[(k-1)/f_s, k/f_s]$ such that

$$y_i[k] = \int_{(k-1)/f_s}^{k/f_s} x_i(t)\Phi_i(t)dt \quad (k = 1 \cdots Tf_s). \tag{5}$$

This random mixing operation can be interpreted as a linear system which transforms the continuous-time signal $x_i(t)$ into a discrete sequence of compressed samples $y_i[k]$. These compressed samples can now be directly digitized at a lower sampling frequency f_s using a less sophisticated ADC such that the undersampling rate (or compression factor) is $N = 2f_{\mathrm{Nyq}}/f_s$. Fourth, after the digitized measurements y_i have been acquired, we can then reconstruct in post-processing uncompressed waveforms $z_i(t)$ by remixing each digitized compressed measurements y_i with the exact same pseudo-random binary functions-noted $\Phi_i(t)$ initially used for the mixing operation in Eq. (5),

$$z_i(t) = \Phi_i(t) y_i[k] \text{ for } \frac{k-1}{f_s} \le t < \frac{k}{f_s}. \tag{6}$$

Note that the waveforms $z_i(t)$ $(i=1,2)$ have the same duration T as the original analog sensor outputs from both sensors $x_i(t)$ and are effectively discretized at the Nyquist frequency f_{Nyq}. Hence the waveforms $z_i(t)$ can be used to construct a different estimate of the expected value $R_{12}(t)$ of the TM noise cross-correlation [Eq. (2)] which is denoted $\tilde{R}_{12}(t)$ and referred to hereafter as the compressed estimator

$$\tilde{R}_{12}(t) = \frac{1}{T}\int_0^T z_1(\tau) z_2(\tau + t) d\tau. \tag{7}$$

The compression operation described in Eq. (5) for each sensor recording $x_i(t)$ can be generalized by using in parallel M different pseudo-random binary functions $\Phi_i^m(t)(m=1\cdots M)$, instead of a single one.[9] This parallelization strategy would then yield M compressed measurements $y_i^m[k]$ $(m=1\cdots M)$ which could then be coherently recombined after post-processing to yield the uncompressed waveforms $z_i(t)$,

$$z_i(t) = \sum_{m=1}^{M} \Phi_i^m(t) y_i^m[k] \text{ for } \frac{k-1}{f_s} \le t < \frac{k}{f_s}. \tag{8}$$

Note that Eq. (8) reduces to Eq. (6) for $M=1$; and that the final expression for computing the compressed estimator $\tilde{R}_{12}(t)$ given in Eq. (7) remains unchanged when $M>1$. We will demonstrate next that this parallelization strategy (for $M>1$) provides a means to reduce the variance of the compressed estimator $\tilde{R}_{12}(t)$, which by analogy with Eq. (3) is given by

$$\text{Var}\left(\tilde{R}_{12}(t)\right) \approx \frac{\sigma_{z_1}^2 \sigma_{z_2}^2}{2TB}. \tag{9}$$

Quantifying the relationships between the compressed estimators $\tilde{R}_{12}(t)$ [Eq. (7)] and the conventional estimator $\bar{R}_{12}(t)$ [Eq. (1)] is more easily done using discrete notations such that Eqs. (1)–(8) can be expressed in matrix form. To do so, let us represent the original noise recording as discrete sequence $\hat{x}_i[q]$ of $Q = T/(2f_{\text{Nyq}})$ samples and introduce the following block diagonal $MB \times Q$ matrix $\hat{\Phi}_i$:

$$\hat{\Phi}_i = \begin{matrix} \Phi_{i,1} & 0 & \cdots & 0 \\ 0 & \Phi_{i,2} & \cdots & 0 \\ \cdots & \cdots & \cdots & \cdots \\ 0 & \cdots & \cdots & \Phi_{i,B} \end{matrix}, \tag{10}$$

where $B = Q/N = Tf_s$ is the total number of compressed samples for each of the M digitized compressed measurements $y_i^m[k]$ $(k=1\cdots B = Tf_s,\ m=1\cdots M)$. In Eq. (10), the entries of each $M \times N$ sub-matrix Φ_{ib} $(b=1\cdots B)$ are independent and identically distributed random binary variable that takes values $\pm 1/\sqrt{M}$ with equal probability; the factor $1/\sqrt{M}$ being chosen so that the columns of each sub-matrix Φ_{ib}—and hence the columns of the larger matrix $\hat{\Phi}_i$ [Eq. (10)]—have unit norm. Hence in matrix notation, Eq. (4) for the digitized compressed measurements can be rewritten equivalently as

$$\hat{y}_i = \hat{\Phi}_i \hat{x}_i \tag{11}$$

and Eq. (8) for the uncompressed waveforms can be expressed as

$$\hat{z}_i = \hat{\Phi}_i^H \hat{\Phi}_i \hat{x}_i, \tag{12}$$

where the superscript H denotes a Hermitian transpose operation. Using this discrete notation, the conventional correlation estimator $\bar{R}_{12}(t)$ [see Eq. (1)] is given by

$$\bar{R}_{12}(t) = \frac{1}{Q}\sum_{q=1}^{Q} \hat{x}_1[q]\hat{x}_2[q+t] = \langle \hat{x}_1, S^t \hat{x}_2 \rangle, \tag{13}$$

where $\langle \cdots, \cdots \rangle$ is the standard discrete inner product and S^t is a $Q \times Q$ matrix whose action (circularly) shifts a vector $(S^t \hat{x}_i)[q] = \hat{x}_i[q+t]$. The time variable t in Eq. (13) is allowed to be continuous-when t is not an integer, S^t is still well-defined using sinc interpolation such that $\bar{R}_{12}(t)$ can be estimated on an arbitrarily fine grid. Similarly, the compressed correlation estimator $\tilde{R}_{12}(t)$ [see Eq. (7)] is given by

$$\tilde{R}_{12}(t) = \langle \hat{z}_1, S^t \hat{z}_2 \rangle. \tag{14}$$

These discrete notations can be used to first demonstrate that the compressed estimator $\tilde{R}_{12}(t)$ [Eq. (14)] converges towards the same expected value $R_{12}(t)$ [Eq. (2)] as the conventional estimator $\bar{R}_{12}(t)$ [Eq. (13)]. This follows from the independence of the random matrices $\hat{\Phi}_i$ [Eq. (10)] and the fact that $E[\hat{\Phi}_i^H \hat{\Phi}_i] = I_Q$. So for a *fixed* pair of discretizes vectors $\hat{x}_1$ and $\hat{x}_2$, using Eq. (12),

$$E[\tilde{R}_{12}(t)] = E\lfloor x_1^H \hat{\Phi}_1^H \hat{\Phi}_1 S^t \hat{\Phi}_2^H \hat{\Phi}_2 x_2^H \rfloor = x_1^H E\lfloor \hat{\Phi}_1^H \hat{\Phi}_1 \rfloor S^t E\lfloor \hat{\Phi}_2^H \hat{\Phi}_2 x_2^H \rfloor = \langle \hat{x}_1, S^t \hat{x}_2 \rangle. \tag{15}$$

And so, by iterated expectation, for the case of random discretized vectors $\hat{x}_1$ and $\hat{x}_2$,

$$E[\tilde{R}_{12}(t)] = E\big[E[\tilde{R}_{12}(t)|\hat{x}_1, \hat{x}_2]\big] = \frac{1}{Q} E\big[\langle \hat{x}_1, S^t \hat{x}_2 \rangle\big] = R_{12}(t). \tag{16}$$

Equation (16) proves that both the conventional correlation estimator $\bar{R}_{12}(t)$ and compressed estimator $\tilde{R}_{12}(t)$ converge towards the same expected value $R_{12}(t)$.

Let us determine now the relationship between the variance of the compressed estimator $\tilde{R}_{12}(t)$ [Eq. (14)] and the variance of the conventional estimator $\bar{R}_{12}(t)$ [Eq. (13)], as the variance of each estimator determines the level of residual fluctuations in each waveform $\tilde{R}_{12}(t)$ or $\bar{R}_{12}(t)$. To do so, let us assume that $M = 1$ first. In this case, based on Eqs. (11)–(13), it can be seen that each discretized samples of the uncompressed measurement vector $\hat{z}_i$ $(i = 1,2)$ is obtained from the linear combination (or average) of N samples of the noise measurement vector $\hat{x}_i (i = 1,2)$. Assuming these N samples are statistically uncorrelated, then $\mathrm{Var}(\hat{z}_i) = N\mathrm{Var}(\hat{x}_i)$. Now, when $M > 1$, Eq. (8)—and its discretized version Eq. (12)—indicates that the uncompressed measurement vector $\hat{z}_i$ is obtained as an ensemble average of M random projections of the same measurement vector $\hat{x}_i (i = 1,2)$. Thus, compared to the case $M = 1$, this reduces the variance of the uncompressed measurement vector $\hat{z}_i$ by a factor $1/M$ such that

$$\mathrm{Var}(\hat{z}_i) = \sigma_{z_i}^2 \approx \frac{N}{M}\mathrm{Var}(\hat{x}_i) = \frac{N}{M}\sigma_{x_i}^2. \tag{17}$$

Consequently, based on Eqs. (3) and (11), the result from Eq. (17) implies that the relationship between the variance of the compressed estimator $\tilde{R}_{12}(t)$ [Eq. (14)] and the variance of the conventional estimator $\bar{R}_{12}(t)$ [Eq. (13)] is

$$\mathrm{Var}\big(\tilde{R}_{12}(t)\big) \approx \left(\frac{N}{M}\right)^2 \mathrm{Var}\big(\bar{R}_{12}(t)\big).$$

Consequently, in practice, the variance of the compressor estimator $\tilde{R}_{12}(t)$ can be reduced in two different ways to achieve a variance similar to that of the

conventional estimator $\bar{R}_{12}(t)$. First, the variances of both estimators $\tilde{R}_{12}(t)$ and $\bar{R}_{12}(t)$ naturally decrease inversely with the duration of the noise recordings [see Eqs. (3) and (9)]. Thus, one could simply increase the recording duration from T to $T(N/M)^2$ to proportionally reduce the variance of the estimators $\tilde{R}_{12}(t)$ by a factor $(M/N)^2$ provided that time-invariance of the system still holds during this longer recording $T(N/M)^2$. A second approach (which could potentially increase hardware complexity) is to perform the compression operation for each sensor recording $x_i(t)$ using a sufficiently larger number of M compression channels. The main advantage of this parallelization approach would be to yield a compressed estimator $\tilde{R}_{12}(t)$ with potentially the same variance as the conventional estimator $\bar{R}_{12}(t)$ if the number of compression channels M is set equal to the undersampling rate N.

3. Experimental results

The proposed approach was tested experimentally by recording TM noise in the frequency band $B=$[12–25 MHz], with a CMUT ring-array monolithically integrated with complementary metal oxide semiconductor (CMOS) electronics (CMUT-on-CMOS) using the exact same experimental setup and apparatus described in a previous study[4] (see Fig. 1). The arrays elements have an area of $70\,\mu\text{m}\times 70\,\mu\text{m}$ and a self-noise level (estimated at 3 mPa/$\sqrt{\text{Hz}}$ noise pressure at 15 MHz) at the TM noise level of the CMUTs.[4,12,13] The CMUT array was immersed in a 2 mm layer of water and recorded $T=1$ s of TM noise on two selected elements 1 and 2 (Fig. 1) sampled at the frequency $2f_{\text{Nyq}}=100$ MHz (14 bits dynamic range). The water-air interface provides a simple plane reflector above the CMUT array (Fig. 1). Figure 1(b) displays the conventional cross-correlation waveform $\bar{R}_{12}(t)$ between receivers 1 and 2 [see Eq. (1)] which shows a clear symmetric and broadband arrival centered at $\pm 2.6\,\mu$s—corresponding to the echo signal from the interface. Physically, the temporal symmetry of the coherent arrivals of $\bar{R}_{12}(t)$ results from the accumulation over the recording duration T of an equal number of noise sources propagating successively both from sensor 1 to sensor 2 and vice versa. The large broadband peak centered at $t=0$ s is the result of electronic noise recorded on both CMUT elements and does not correspond to a specific acoustic path in the water layer.[4]

The compressed estimator $\tilde{R}_{12}(t)$ [see Eq. (6)] was computed in post-processing by first mixing the same 1 s-long noise recordings [used to compute the conventional estimator $\bar{R}_{12}(t)$] with a single pseudo-random binary function (i.e., $M=1$) for increasing undersampling rate $1\leq N\leq 25$. Compared to the conventional correlation in the upper plot of Fig. 1(b), the lower plot shows the compressed estimator $\tilde{R}_{12}(t)$ obtained here using an undersampling rate of $N=10$ of the original noise recordings (i.e., those with an effective sampling frequency of only $f_s=10$ MHz). The water-interface echoes at $\pm 2.6\,\mu$s are still clearly visible in the lower plot but, as expected, there are larger residual temporal fluctuations around the coherent arrival when compared to the upper plot caused by this tenfold decrease of the sampling frequency from $2f_{\text{Nyq}}=100$ MHz down to $f_s=10$ MHz. The standard deviations [i.e., square root of the variances of the conventional estimator $\bar{R}_{12}(t)$ and compressed estimator $\tilde{R}_{12}(t)$] are estimated from the root-mean-square value of their residual temporal fluctuations in a time window Δt ($3.5\,\mu\text{s}<|t|<5\,\mu$s) outside of the main coherent arrival.[10,11] Figure 1(c) shows that the ratio of the standard deviation of the compressed estimator $\tilde{R}_{12}(t)$ to the standard deviation of the conventional $\bar{R}_{12}(t)$ increases proportionally to the undersampling rate $1\leq N\leq 25$, thus confirming the aforementioned theoretical predictions.

4. Conclusions

Overall, this TM noise-based ultrasonics technique may allow for the close integration of micro-engineered passive (thus low-power) ultrasonic transducers within various ultrasonic sensing or imaging applications. Furthermore, this study demonstrated that the correlations of high-frequency TM noise can be obtained using sub-Nyquist

sampling frequency. This provides a means to relax the ADC sampling requirements for synchronous recordings of high-frequency TM noise on multiple receivers as well as potentially reduce power consumption by using slower ADCs.

Acknowledgment

This work was supported by NSF Grant No. ECCS-1202118.

References and links

[1]R. L. Weaver and O. I. Lobkis, "Ultrasonics without a source: Thermal fluctuation correlations at MHz frequencies," Phys. Rev. Lett. **87**, 134301 (2001).
[2]R. Weaver and O. Lobkis, "On the emergence of the Green's function in the correlations of a diffuse field: pulse-echo using thermal phonons," Ultrasonics **40**(1–8), 435–439 (2002).
[3]E. Larose, O. I. Lobkis, and R. L. Weaver, "Passive correlation imaging of a buried scatterer," J. Acoust. Soc. Am. **119**, 3549–3552 (2006).
[4]S. Lani, S. Satir, G. Gurun, K. G. Sabra, and F. L. Degertekin, "High frequency ultrasonic imaging using thermal mechanical noise recorded on capacitive micromachined transducer arrays," Appl. Phys. Lett. **99**, 224103 (2011).
[5]G. Gurun, M. Hochman, P. Hasler, and F. Degertekin, "Thermal-mechanical-noise-based CMUT characterization and sensing," IEEE Trans. Ultrason., Ferroelectr. Freq. Control **59**(6), 1267–1275 (2012).
[6]A. Eftekhari, J. Romberg, and M. B. Wakin, "A compressed sensing parameter extraction platform for radar pulse signal acquisition," IEEE Trans. Inf. Theory **59**(6), 3475–3496 (2013).
[7]J. A. Tropp, J. N. Laska, M. F. Duarte, J. K. Romberg, and R. G. Baraniuk, "Beyond Nyquist: Efficient sampling of sparse bandlimited signals," IEEE Trans. Inf. Theory. **56**(1), 520–544 (2010).
[8]M. Mishali and Y. C. Eldar, "From theory to practice: Sub-Nyquist sampling of sparse wideband analog signals," IEEE J. Sel. Topics Signal Process. **4**(2), 375–391 (2010).
[9]J. Yoo, C. Turnes, E. B. Nakamura, C. K. Le, S. Becker, E. A. Sovero, M. B. Wakin, M. C. Grant, J. Romberg, A. Emami-Neyestanak, and E. Candes, "A compressed sensing parameter extraction platform for radar pulse signal acquisition," IEEE J. Emerg. Sel. Topics Circuits Syst. **2**(3), 626–638 (2012).
[10]R. L. Weaver and O. I. Lobkis, "Fluctuations in diffuse field–field correlations and the emergence of the Green's function in open systems," J. Acoust. Soc. Am. **117**, 3432–3439 (2005).
[11]K. G. Sabra, P. Roux, and W. A. Kuperman, "Emergence rate of the time-domain Green's function from the ambient noise cross-correlation function," J. Acoust. Soc. Am. **118**, 3524–3531 (2005).
[12]G. Gurun, J. Zahorian, P. Hasler, and L. Degertekin, "Thermal mechanical noise based characterization of CMUTs using monolithically integrated low noise receiver electronics," in *2010 IEEE Ultrasonics Symposium (IUS)* (IEEE International, San Diego, CA, 2010), pp. 567–570.
[13]G. Gurun, P. Hasler, and F. L. Degertekin, "Front-end receiver electronics for highfrequency monolithic CMUT-on-CMOS imaging arrays," IEEE Trans. Ultrason., Ferroelectr. Freq. Control **58**(8), 1658–1668 (2011).